

Hyogo BL (BL24XU)

Junji MATSUI
Yasushi KAGOSHIMA
Yoshiyuki TSUSAKA
Yoshio KATSUYA
Muneyuki MOTOYAMA
Yoshio WATANABE
Kazushi YOKOYAMA
Kengo TAKAI
Shingo TAKEDA
Jun-ichi CHIKAWA

1. Introduction

Construction of the Hyogo beamline as a first contract beamline has progressed favorably at BL24XU and is soon coming into the status of beamline commissioning. First visualization of the specific light pattern from an in-vacuum type "Figure-8" undulator [1] for the hard X-ray region has been recently achieved during the undulator and the front end channel commissioning. It is expected that one optics hutch and three experimental hutches will undergo a geometrical survey and radiation security inspections in near future. At the initial experimental stage after the transport channel commissioning, beam adjustments will be performed in each hutch.

2. Beamline

The *in-vacuum* type Figure-8 undulator, which provides both horizontally and vertically polarized X-rays, have been installed in this beamline. A number of periods and a length of period are 172 and 26 cm, respectively. The horizontally/vertically polarized X-rays can be obtained with integer/half-odd-integer harmonics. The front end channel made of SPring-8 standard components has been also installed by the end of February 1998. Since some of those components cannot stand the high heat load by the intense beam from the undulator, new components which are under development will be installed in this summer.

The construction of radiation shield hutches for the optics and experimental

hutches, have been completed. All of the transport channel components and three double-crystal monochromators (A, B and C) are placed in the optics hutch as seen in Fig.1. Water-cooled slits and view ports are installed at upstream and downstream sites of each monochromator.

In order to reduce the intensity of higher order harmonics, a 40-cm-long Rh-coated mirror is placed at upstream of the experimental hutch A. To restrain the high energy gamma rays, a white shutter is put at downstream of the monochromator C.

Interlock system controllers, which permit the independent operation of three experimental hutches, are placed on the upper deck of the optics hutch.

3. Monochromators

3-1 Installation of Monochromators

Two identical upstream monochromators (A and B) with diamond crystals adopt so-called "Toroika" conception to perform simultaneously three experiments for different purposes. The first crystal acts as a beam splitter taking the Laue case arrangement. X-rays with the photon energy satisfying the Bragg condition are reflected toward the second crystal, while the remaining amount of X-rays transmit the first crystal and enter into the next monochromator. The second crystal takes the Bragg case arrangement and leads the monochromatized X-rays into the respective experimental hutches. A goniometer of the first crystal is mounted on a high precision linear stage being movable parallel to the beam axis as far as 1200 mm so that the photon energy can be tuned. In the monochromators A and B, a diamond crystal (~9 mm wide, ~9 mm high and 0.3 mm thick) is mounted on a water-cooled copper holder. The thermal contact between the crystal and the holder will be made by using Gd-In liquid alloy.

The monochromator C is of the silicon double-crystals. It has a mechanism with which the first crystal can be put on or remove from the beam axis so that either 'monochromatic' or 'white' experimental mode can be operated. The monochro-

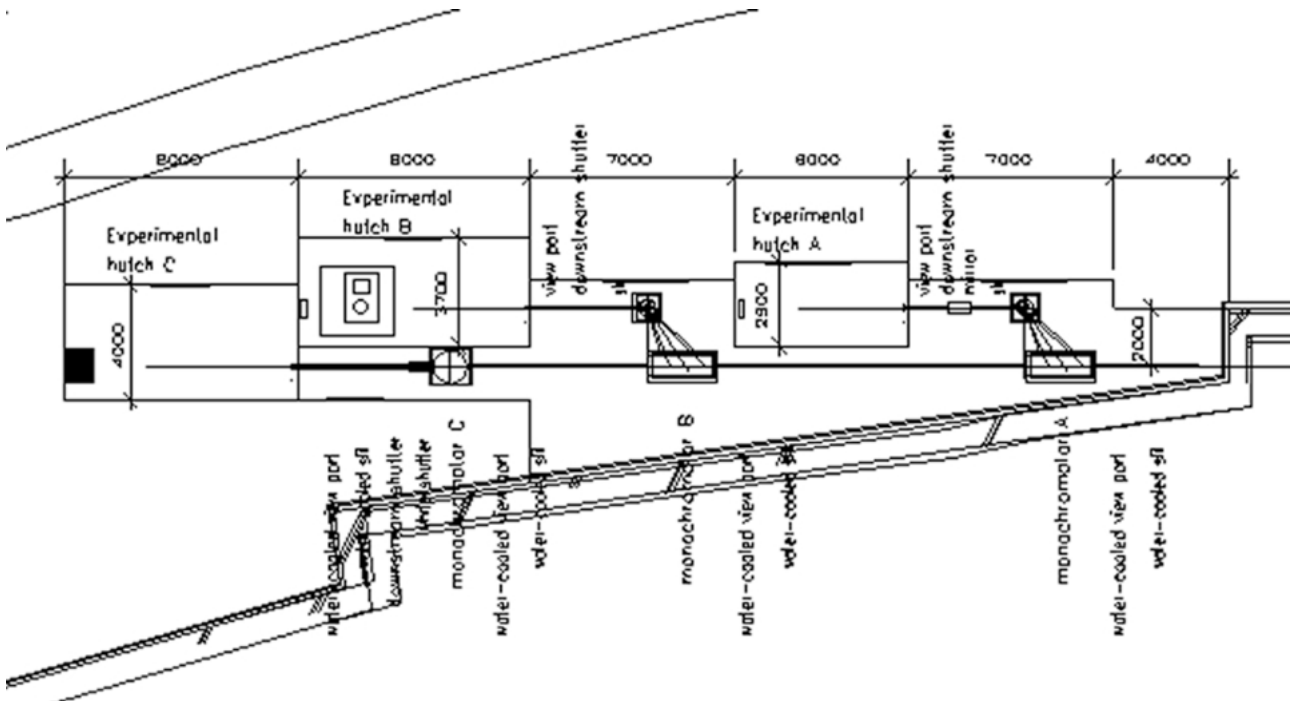


Fig.1 Plane view of Hyogo beamline.

monochromator C adopts a so-called “fin-cooling [2] method. The surface power density impinging to the first silicon crystal in the case of a standard mode ($K_x=1.31$, $K_y=1.12$, $E_1=9.4$ keV) is estimated to range from 0.2 to 1.6 W/mm² @20mA corresponding to a tunable photon energy of the monochromator ranging from 37.8 to 4.7 keV. The crystal will be well cooled under those conditions.

The first crystals of all monochromators and the second crystal of the monochromator C are water-cooled. The temperature and the flow rate of the cooling water are controlled by using a closed-circuit chiller.

The specifications of monochromators are summarized in Table.1. Schematic drawings of the monochromators are shown in Fig.2 and Fig.3.

3-2 Characterization of Diamond Crystals

The quality of the diamond crystals is a key issue to make our Toroika system successful. The development of diamond crystals has started as a joint program of SPring-8 project team and Sumitomo Electric Industries (SEI) [3]. The diamond crystals with a (100) or a (111) surface were characterized by the use of rocking curve measurements, reciprocal lattice mapping and Lang topography method. The full

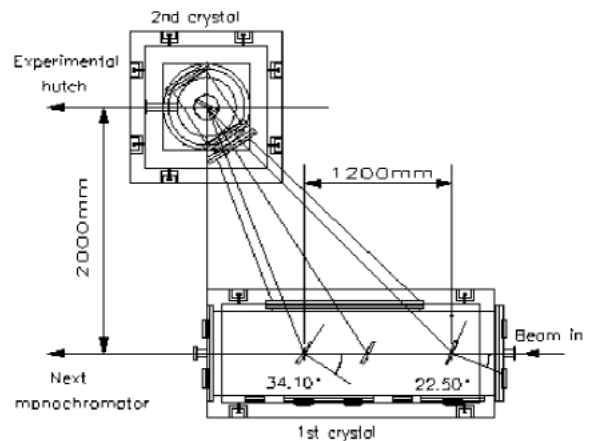


Fig.2: Plane view of monochromator A or B.

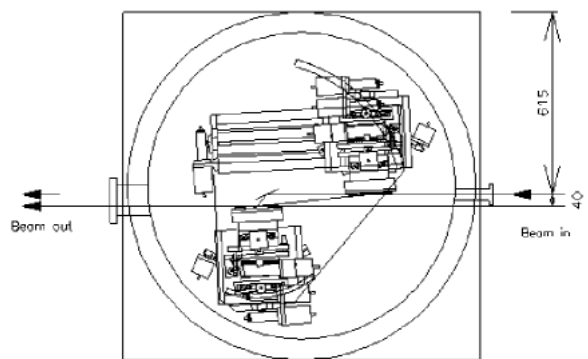


Fig.3 Plane view of monochromator C.

Table.1 Specifications of monochromators.

Monochromator	A	B	C
Crystal	Diamond		Silicon
Bragg angle (deg.)	22.5 ~ 34.1		3.0 ~ 25.0
Offset distance (mm)	2000		40
Reflection plane	{400}	{220}	{111}
Energy range (keV)	12.40 ~ 18.17	8.77 ~ 12.85	4.7 ~ 37.8

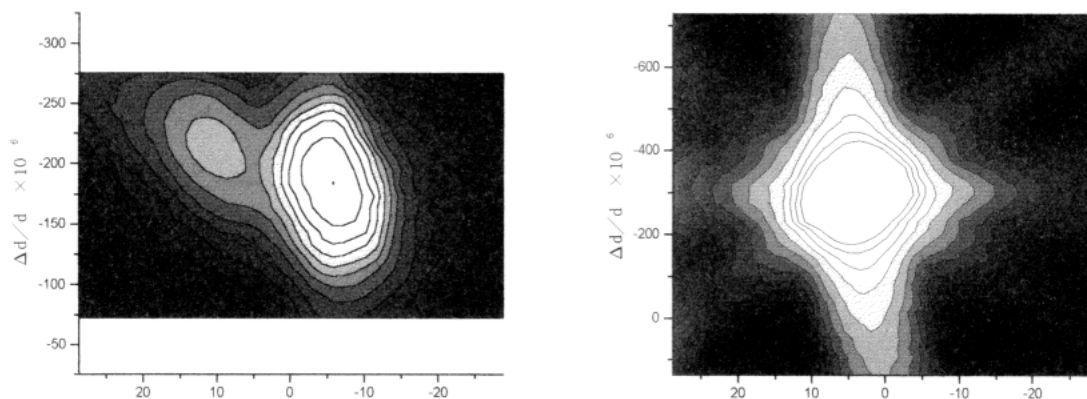


Fig.4 Reciprocal lattice maps for (left) (100) and (right) (111) planes of diamond crystals.

widths of the half maximum of the rocking curves at the X-ray energy of 8.04 keV were measured to be 6.2 arcsec and 6.1 arcsec for 400 and 111 Bragg reflection, respectively. These values are 1.5 and 1.2 times larger than the theoretical ones. Fig.4 (left) shows a 400 reflection reciprocal lattice mapping result around a position of 2 mm away from the center of the (100) crystal. A sub-peak of about 15 arcsec leaning to the main peak is clearly seen in this figure. No sub-peaks can be seen in 111-reflection reciprocal lattice maps as typically shown in Fig.4 (right). In addition, some streaky intensity distribution due to a dynamical effect of the X-ray diffraction, being elongated in the radial direction from the reflection point, is clearly seen, which means that crystallinity of (111) planes is more perfect than that of (100) planes.

It has also been clarified that the diamond crystals include some defect bundles inside the crystals. We expect, however, that they do not give rise to any serious problems for monochromatization as far as a central region of the crystal is used for the reflection. Those characterization results including an information of the defects in the diamond crystals will appear some-

where.

4. Experimental Hutch A

In order to facilitate protein crystallography in industrial fields, the hutch A is dedicated to ordinary X-ray diffraction experiments for small protein crystals. X-rays with the energy of about 14.4 keV is selected from the 1.5th harmonic of the Figure-8 undulator. After collimating the X-rays by a slit, a fiat mirror excludes the higher harmonics. The X-ray wavelength is chosen to be appropriate for single isomorphous replacement method with anomalous scattering (SIRAS) for platinum or mercury derivatives.

An oscillation camera with an imaging plate (IP) detector and a one-axis goniometer are installed for data collection. The IP detector is Rigaku R-AXIS4 of which IP size is 300×300 mm². Distance from the crystal to the detector can be adjusted in the range from 80 to 500 mm.

In order to minimize radiation damage of crystals from the incident X-ray beam, a cryo-cooling system is installed. The temperature is controlled within 93-473 K.

Table. 2 Specifications of analytical equipment.

Sample Chamber	Chamber	Vacuum	< 0.06 Torr	
	Sample Stage	Sample Size	40(X) × 40(Y) × 10(Z) mm	
		Accuracy	ω	< 0.001 deg
			χ	< 0.001 deg
		ϕ	< 0.05 deg	
PIN-SSD	XRD mode	Radius	150 mm	
		Position Resolution	< 0.01 deg	
	TXRF mode	Energy Range	2 ~ 10 keV	
		Energy Resolution	$E/\Delta E > 20$	
Curved PSPC	XRD	Radius	250 mm	
		Position Resolution	< 0.08 deg	
		Time Resolution	< 5 msec	
Flat PSPC combined with analyzing crystals	WDXRF	Energy Range	2 ~ 10 keV	
		Energy Resolution	$E/\sim E > 2500$	
		Position Resolution	< 200 μm	
		Distance from Sample	1400 mm	

5. Experimental Hutch B

5-1 X-ray Surface Analysis

An X-ray surface analysis equipment is prepared mainly for inorganic material analyses. The equipment is designed to analyze elemental compositions, chemical states and structures simultaneously by means of fluorescent and diffracted X-ray intensity measurements in a grazing incidence geometry. It consists of four major instrumental parts; a sample chamber, a solid state detector (SSD), a curved position-sensitive proportional counter (PSPC) and a flat PSPC combined with analyzing crystals (WDXRF; wave-dispersive X-ray fluorescence analysis). The basic characteristics of each part are shown in Table.2.

In addition to the ordinary compositional and structural analyses, highly resolved energy and polarization of characteristic X-rays emitted from the sample can be measured by means of a flat crystal combined with a flat PSPC spectrometer. In order to notice the horizontally polarized X-ray beams, the spectrometer can be set at any angles with respect to the incident beam. Since few works on polarized X-ray emission phenomena have been carried out, it is one of the experimental purposes to investigate the polarization effect in the hard X-ray region with the use of this equipment.

5-2 *in-situ* Observation of Growing Crystal Surfaces

Compound semiconductors are very useful materials in terms of optical and electronic devices. Those device structures are usually grown by organometallic vapor phase epitaxy (OMVPE) and molecular beam epitaxy (MBE). In OMVPE, the carrier gas (typically H₂) incorporating a small concentration of reactants flows passing on heated substrate, and crystal growth occurs on the substrate surface by decomposing the reactants. However, little is known about the detailed growth mechanism or atomic arrangements during the epitaxial growth because those processes go under atmospheric or near-atmospheric pressure conditions.

In order to investigate a relationship between the surface/interface atomic arrangements and the device characteristics, an *in-situ* grazing incidence X-ray diffraction (GIXD) apparatus is now being developed. A schematic diagram of the reactor which is installed in a downstream half of the hutch B is shown in Fig.5.

The reactor employs a vertical flow design in which the source gases are introduced at the top and flow down to the heated sample surface. X-rays impinge on the surface at a small grazing angle (α) and scattered X-rays are detected at an in-plane scattering angle (2θ) and at an

out-of-plane scattering angle (beta).

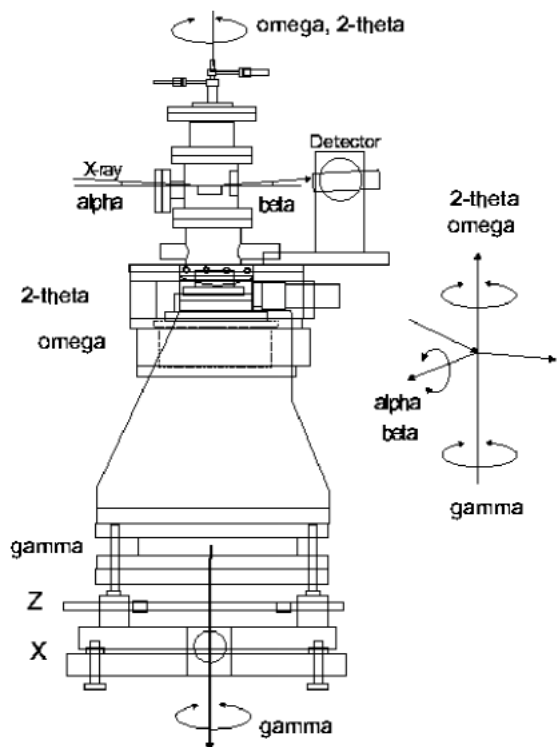


Fig. 5: Side view of in-situ grazing incidence X-ray diffraction (GIXD) apparatus.

6. Experimental Hutch C

In the experimental hutch C (8 m long and 4 m wide, being also called as 'optics hutch B' because of severe radiation shield structures for treatment ability of white X-rays), three anti-vibration tables are installed. On each of those tables, different kinds of Z-stages and goniometers have been prepared. Each goniometer can be placed on any Z-stages of any tables depending upon the experimental purposes. Formation of a focussed microbeam or a quasi-plane-wave microbeam of less than a few μm^2 in size will be primarily tried. Those microbeams are expected to be useful for crystallographic characterization or strain distribution measurement at very local parts in the materials. Fig.6 shows a typical setup on a table for forming the focussed microbeam with the use of a capillary.

By adopting successive and asymmetric reflections, for instance, a combination of $11n$ ($n \geq 5$, odd numbers) reflections from Si(001)-surface crystals, we can obtain a quasi-plane-wave X-rays of a small or a large

beam width depending upon an optical geometry of the reflections (*i.e.* asymmetric factors). The small beam will be useful for delineation of so-called reciprocal lattice maps (like Fig.4) from one local portion to another in a strained single crystal surface, while the large beam will be used for getting an image of a wide crystal area such as strain-sensitive topography.

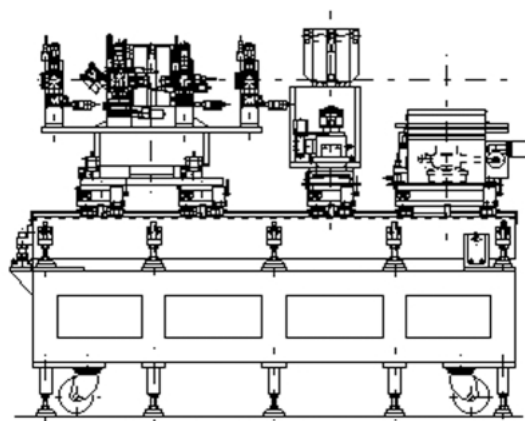


Fig. 6: Side view of microbeam formation table.

In this hutch, photo-reaction experiments for new material creation through inner-shell excitations by the white X-ray irradiation will also be performed. Many scientists from more than six groups totally will join the collaborative works which will be carried out in hutch C.

7. Acknowledgements

Prof. M. Ando, Drs. H. Sugiyama, X. Chan and K. Hyodo of Photon Factory are acknowledged for the beamline design at the initial stage of this plan. Drs. Y. Ono, T. Kaneyoshi and other persons of Hyogo Prefectural Institute of Industrial Research are joining us to carry out and discuss the studies using the equipments installed in hutches A and B. Several persons of NTT also contribute to preparation of the in-situ observation system for OMVPE growth in hutch B. We would like to thank Dr. S. Kimura in NEC Corporation for collaborating in estimation of the diamond crystals.

Drs. H. Kamitsubo, H. Ohno, T. Ueki, S. Shimomura, H. Kitamura, T. Ishikawa, J. Mizuki and others of JAERI-RIKEN

SPring-8 Project Team are greatly appreciated for their valuable suggestion and support for construction of the Hyogo beamline. Finally, it should be noted that Messrs. T. Okada, H. Ochiai and T. Sakaki of Hyogo Prefecture have made much effort for budgetary and supporting works.

References

[1] T. Tanaka and H. Kitamura, Nucl. Instr. Meths. **A364**, 368 (1995).

[2] T. Oversluzen, T. Matsushita, T. Ishikawa, P. M. Stefan, S. Sharma and A. Mikuni, Rev. Sci. Instrum. **60**, 1493 (1989).

[3] T. Ishikawa, SPring-8 Annual Report 1996, 30 1997 .